NASA

NASA Contract # NNC10BA06B

Task # NNC10TA64T

RTAPS

Task Order: ERA Advanced Core Compressor Technology Program

David Lurie, Andy Breeze-Stringfellow, Stuart Wilson, Richard Obear, Ki Sohn, Hyoun-Woo Shin

GE Aviation

May 2014

Final Report

NASA
Glenn Research Center
21000 Brookpark Road
Cleveland, OH 44135

Table of Contents

Index of Figures

List of Tables

Symbols List

ERA	=	Environmentally Responsible Aviation
HPC	=	High Pressure Compressor
PR	=	Pressure Ratio
RTAPS	=	Research and Technology for Aerospace Propulsion Systems
SFC	=	Specific Fuel Consumption
SOTA	=	State Of The Art
PS	=	Static Pressure
PT	=	Total Pressure
TT	=	Total Temperature
LE	=	Leading Edge
TE	=	Trailing Edge
IGV	=	Inlet Guide Vane
R1	=	Rotor 1
S1	=	Stator 1
R2	=	Rotor 2
S2	=	Stator 2
VSV	=	Variable Stator Vane
1-Stg	=	1 Stage Configuration
2-Stg	=	2 Stage Configuration
OTR	=	Over The Rotor
ID	=	Inner Diameter
OD	=	Outer Diameter
ALF	=	Aft Looking Forward
TDC	=	Top Dead Center
Circ	=	Circumferential
NC	=	Corrected Speed
ALPHAM	=	Meridional Swirl Angle

All corrected conditions are corrected to standard day where:
Pref = 14.696 psi
Tref = 518.67 R

Acknowledgements

There were a lot of people whose work made this test campaign a success. The authors would like to thank the following people from General Electric, John Davis and Chuan He for their work for coordinating and acquiring the essential detailed traverse data, Tod Steen for his support during the test on rotor balancing, Jeff Greatorex for instrumentation in the build up to and during the test, Craig Burns for overseeing the mechanical design of the rig, and Tony DiPietro for working the aero test design in the pre-test stage. We would also like to acknowledge and thank the people at the NASA Glenn Research Center and their contractors for the great support they provided to the test. The authors would like to thank John Fabian (formerly GRC), Mark Celestina (GRC), Sameer Kulkarni (GRC), Ken Suder (GRC), Dave Althausen (Vantage Partners, LLC), Julia Stephens (GRC), Alicia Graham (GRC), and especially Sue Prahst (ZIN TECHNOLOGIES INC) for their support pre, during and post test. There are many more people to thank, and the authors apologize to anyone left off the above list.

Purpose

As part of the NASA Integrated Systems Research Program, Environmentally Responsible Aviation Project, NASA GRC and GE Aviation have partnered to investigate the technology barriers associated with improved fuel economy of large gas turbine engines. Crucial to improving fuel economy is the increase in Pressure Ratio (PR) of the core compressor.

General Electric is in the process of defining new advanced technology engine concepts and related engine architectures for both commercial and military subsonic and supersonic flight applications. These new concepts and architectures offer the potential of providing substantial improvements in mission fuel burn, emissions, and noise levels relative to SOTA engines and support the needs and goals of future Air force, Navy, and NASA aircraft systems. A key aspect of many of these new engine concepts is an ultra high pressure ratio core compressor. Current SOTA engines such as the GENx utilize a 23:1 class pressure ratio core compressor to achieve an overall pressure ratio in the 50:1 class. Future engines with overall pressure ratios in the 70– 80:1 class will need core compressors with pressure ratios in the 30:1 class. These single spool, ultra high pressure ratio compressors will have inherent challenges. The goal of this work is to provide a dedicated component test vehicle to study the very challenging compressor front stage performance and operability issues that arise in these aggressive machines. With a view to providing highly detailed aerodynamic data that will provide, subject to the rights restrictions for test data afforded under NASA Contract NNC10BA06B/NNC10TA64T, an industry standard data set for CFD validation.

Background

Improvements in the front block of the core compressor are required to increase the pressure ratio (and therefore the thermal efficiency) of the engine core. These improvements are required to meet the aggressive fuel burn goals of NASA's Environmentally Responsible Aviation (ERA) project for the N+2 timeframe.

GE is developing compressors in the 30:1 pressure ratio class to satisfy the requirement for ultra high pressure ratios on a single spool. GE has found these compressors to have some significant challenges. The most significant aerodynamic concern is matching and performance of the front two or three transonic compressor stages. In order to get this pressure ratio in a limited number of stages the front stages of the machine are high speed and may be high reaction and hence the rotor relative Mach numbers over the first few stages are high. The experience is that these types of stages are difficult to match together because they have vertical speed characteristics and they operate efficiently over relatively small flow ranges. Any unexpected losses in the system result in significant stage mis-matches that further degrade the performance of the machine. To date the analytical CFD tools have not been able to reproduce all the loss mechanisms seen in the test data. In addition to the performance challenges, the very high loading on a single spool means that, at part speed the front stages of the compressor get throttled significantly and create a significant part speed operability challenge to the overall compressor.

This work also addresses development of the following advanced turbomachinery concept features defined in NASA's RFP under 2.1.2 High Power Density Engine Turbomachinery:

(b) Low loss variable inlet guide vanes, rotors, stators, transition ducts, seals, and secondary flow systems and struts
(f) Aerodynamic stage matching technologies for efficient multistage transonic compressors
(j) Other features resulting from current system studies

GE and NASA have both experienced lower levels of efficiency from front stages of highly loaded compressors than would have been expected or indeed been predicted by state of the art CFD. This inability to predict the losses makes achievement of the desired stage matching currently very challenging. This rig was designed to be the tool that allows identification of the as yet not fully understood high speed loss sources. To these ends the rig was designed to facilitate the taking of large amounts of unsteady pressure, hot wire and PIV data (although the PIV data was not obtained due to budget and time constraints). The data will eventually provide a new reference data set, subject to the rights restrictions for test data afforded under NASA Contract NNC10BA06B/NNC10TA64T, to the aerospace industry (similar to rotor 37) as a benchmark for the testing and calibration of CFD tools and the understanding of phenomenon related to high stage loading, transonic blade row performance and matching at both high and low rotor speeds.

Additionally high spool pressure ratio compressors have significant operability and aeromechanical challenges in the front stages of the rotor at low compressor speeds and pressure ratios when the inlet flow coefficient to the compressor becomes very low. Under these conditions there are significant flow separations in the front stages and the best means to achieve good stall margin and low aeromechanical responses is not clear. It is expected that this rig program will also help understanding of the flow physics at these operating conditions and allow better design strategies in future compressors. Although these issues are not being pursued under the work package being reported here, they are the subject of follow on work.

By addressing, understanding and solving the challenges associated with aerodynamic losses and stage matching GE believes that future core compressors can be designed with higher efficiency, thereby enabling improvement in mission fuel burn.

Technical Approach

This program is centered around the development of compressor front stage technology as an enabler for higher pressure ratio more efficient compressors. The thermal efficiency of a Brayton cycle engine is directly related to the overall cycle pressure ratio. A significant amount of work is currently being done to improve the propulsive efficiencies of commercial engines, but this path should not be followed blindly without consideration of the thermal efficiency of the cycle. Current commercial engines run at overall cycle pressure ratios of 30-45 but study engines are now looking at overall pressure ratios in the 60-70+ range. One key enabler to such high cycle pressure ratios are compressors with significantly higher spool pressure ratios.

This test program aims to investigate the current technical barriers to high stage loading front stages suitable for a very high cycle pressure ratio compressor. The program will test the front 2 stages of an experimental GE compressor, the Tech56 rig3. This machine has high stage loadings achieved through high stage reaction. This machine did not meet its pre-test high speed efficiency goals because of losses in the front 2 stages of the compressor. These losses were not fully understood and have not been predicted by sophisticated compressor CFD simulations. This included full wheel, multi-blade row unsteady CFD of compressor IGV thru rotor 2.

The plan is to run this machine as a single stage machine initially to fully characterize and understand stage 1. Then run it in the 2-stage configuration. Advanced diagnostic instrumentation is planned for the 2-stage configuration to fully characterize the interaction effects of the rotor 2 upstream traveling shock system on stator 1 and on the wakes from stator 1 and rotor 1. The goal being to fully understand and model the loss mechanisms, thus permitting the development of front stages that mitigate the identified losses and permit the machine to reach its target level of efficiency.

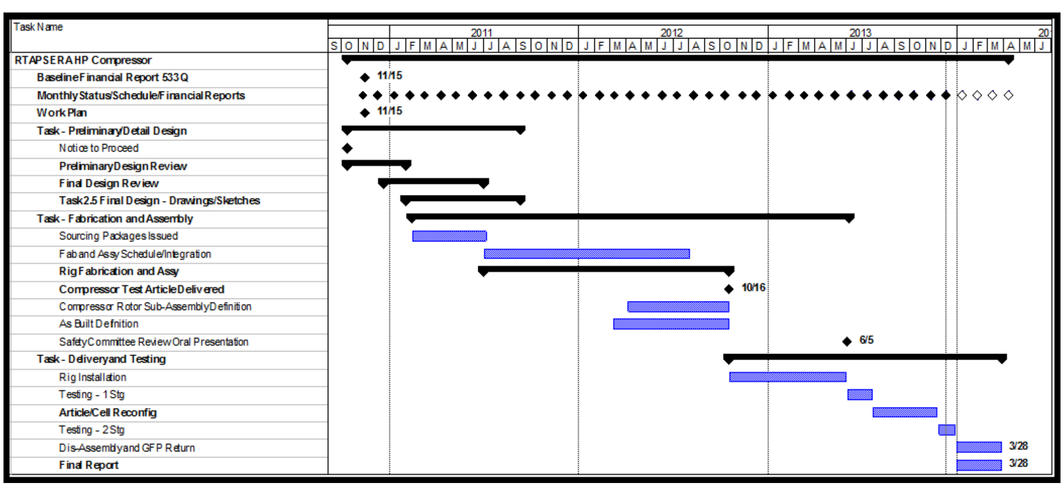

Figure 1 Program Schedule

Test Rig Design

The compressor vehicle used in this work comprises the first 2 stages of the GE's Tech56 rig3 high stage loading compressor. This compressor rig configuration was chosen because it is GE's highest loading compressor configuration tested to date and provides useful data in understanding the issues that may be encountered with future high stage loading compressors that may well be required for tomorrows ultra-high pressure ratio cycles.

The test rig is designed to investigate the source of high front stage loss in the Tech56 rig 3. In order to isolate the first stage from any interaction loss effects caused by the downstream stage, the rig has the unique capability to operate in a 1-stage (1 Stg) or 2-stage (2 Stg) configuration. Figure 2 shows the rig in the respective 1 Stg and 2 Stg capable configurations.

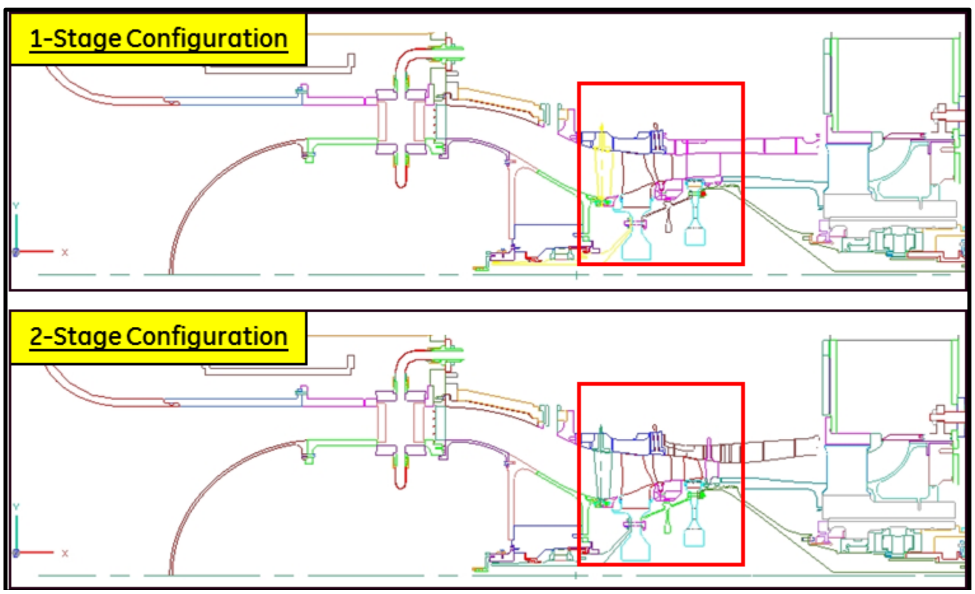

Figure 2 1-Stage and 2-Stage Rig Configuration

The test rig contains detailed instrumentation to measure pressures and temperatures. The inlet flowpath contains instrumentation to measure wall static pressure and the inlet boundary layer as well as a distortion screen to generate the desired inlet PT profile at the IGV LE. Also there is access to perform radial traverses upstream of the strut LE. Figure 3 shows this instrumentation layout.

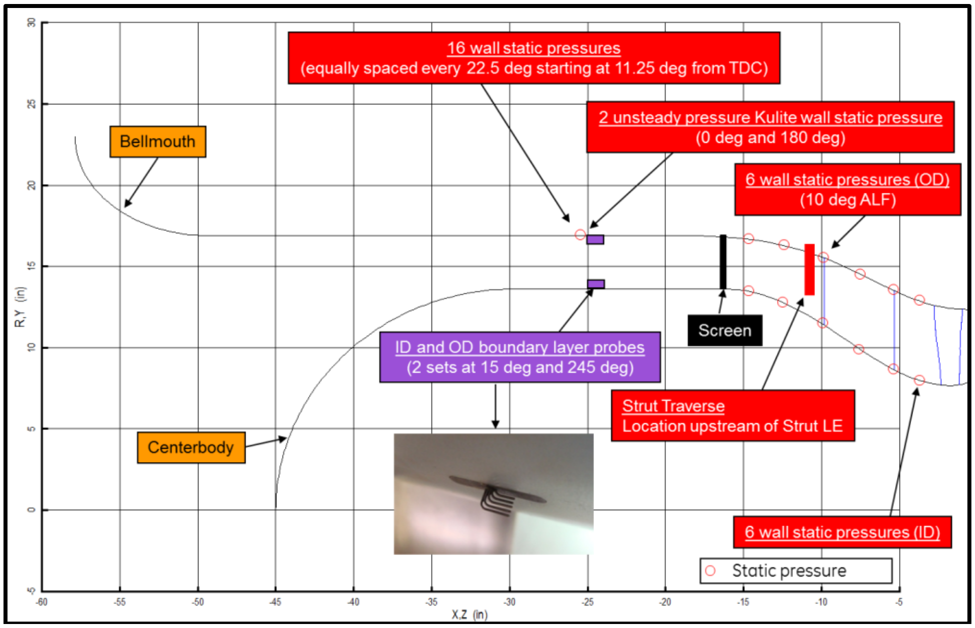

Figure 3 Rig Inlet Flowpath Instrumentation

The test rig contains PT/TT rakes in the inlet at plane 25 and in the exit downstream of the last stator in plane 30.

There are 5 inlet rakes placed in between the 5 struts in the gooseneck. The inlet rakes, shown in Figure 4, contain 5 immersions that measure total pressure and temperature. There are also 5 static pressure measurements in the case in the plane of the inlet rake.

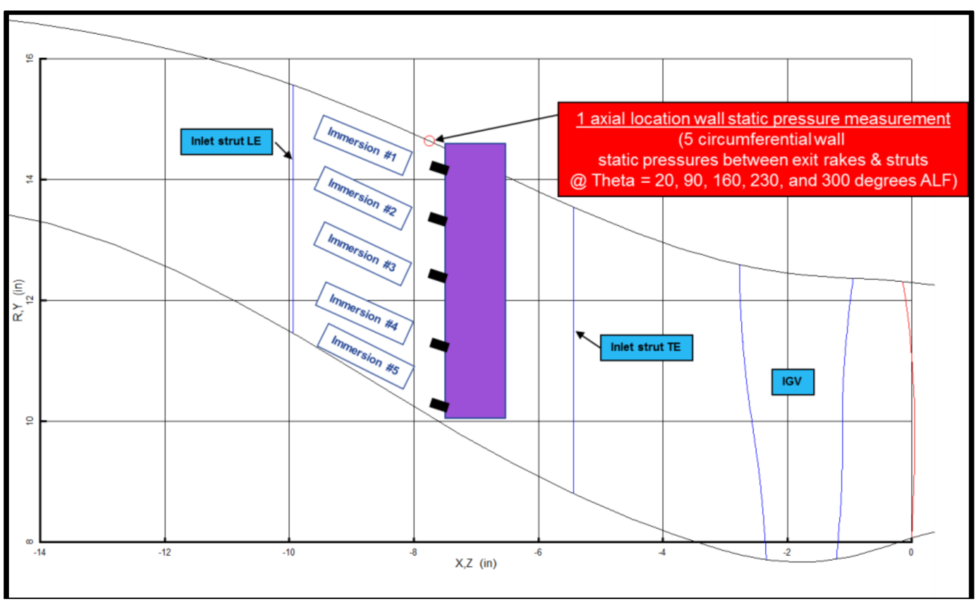

Figure 4 Inlet PT/TT Rakes

There are 2 sets of plane 30 exit rakes configured to support the 1-stg and 2-stg configuration. The Plane 30 exit rakes configurations are shown in Figure 5 and Figure 6.

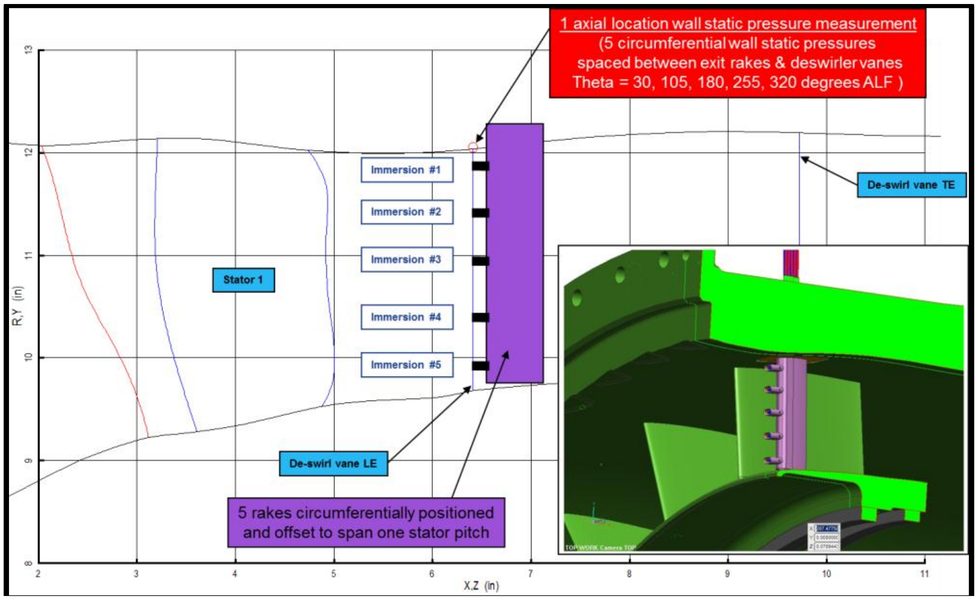

Figure 5 Plane 30 Exit Rakes – 1-Stage Configuration

In the 1-stg configuration, there are 5 rakes spaced between the deswirler vanes, and each rake measures 5 immersions of total pressure and temperature. The exit rakes are positioned circumferentially such that they are each in different locations with respect to the S1 TE, resulting in equally spaced measurements across one stator pitch. There are also 5 casing wall static pressure taps around the circumference located in the middle of a deswirler vane passage.

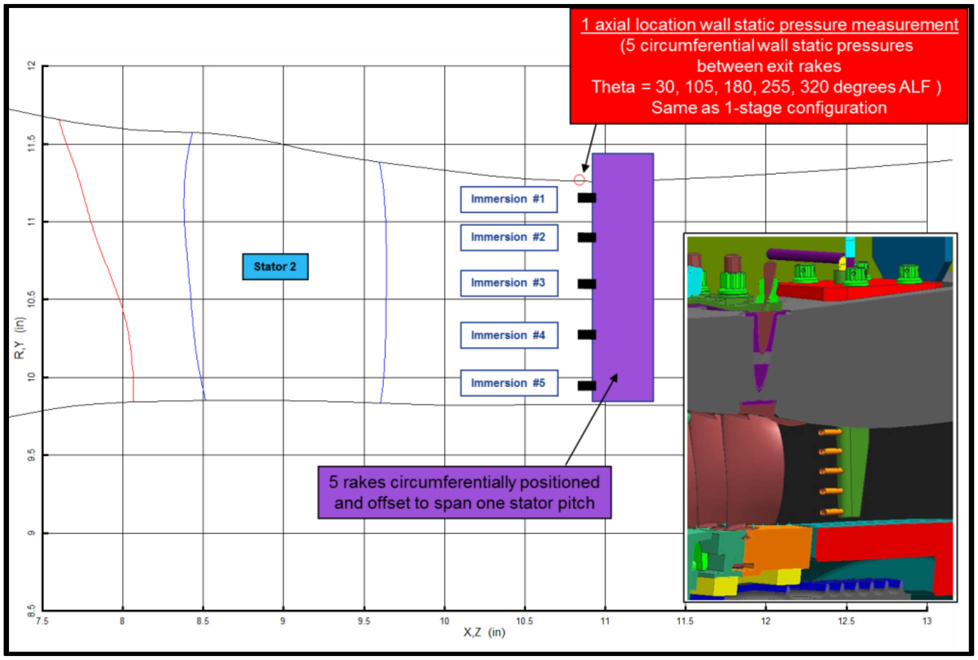

Figure 6 Plane 30 Exit Rakes – 2-Stage Configuration

In the 2-stg configuration, the exit rakes are placed behind the S2 TE, and are also positioned to measure across one stator pitch. Unlike the 1-stg configuration, there are no deswirler vanes.

In the 2-stg configuration only, there is also a wiper rake, shown in Figure 7

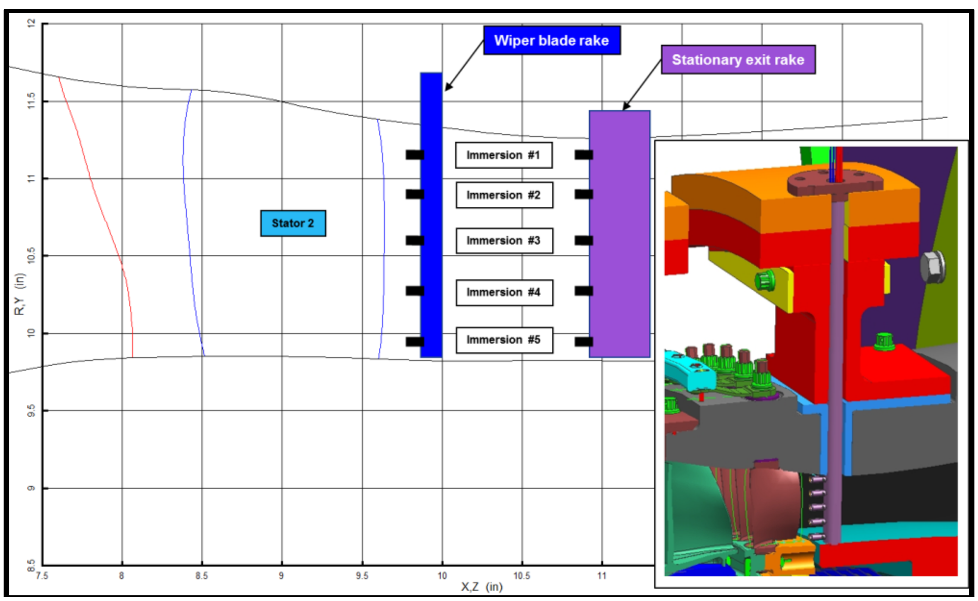

Figure 7 Wiper Rake – 2-Stage Configuration

The wiper rake can be installed behind the S2 TE upstream of the Plane 30 exit rakes and contain 5 immersions that are traversed circumferentially to measure both total pressure and temperature across one S2 pitch.

Table 1 Rake Instrumentation Locations

	Plane 25	Plane 30 (1stg)	Plane 30 (2stg)	Plane 30 (Wiper Rake)
Axial Location	50% chord of Strut	0.83 chords downstream S1	0.95 chord downstream S2	0.13 chords downstream S2
Immersion A	9.2%	9.0%	10.9%	10.0%
Immersion B	27.0%	27.8%	29.8%	29.1%
Immersion C	45.9%	47.3%	49.2%	48.7%
Immersion D	66.2%	67.6%	69.2%	69.0%
Immersion E	88.3%	88.9%	89.7%	89.8%

The axial location and radial immersion of the rake elements are shown above in Table 1.

Both the 1-stg configuration and 2-stg configuration contain similar inter-stage instrumentation, shown in Figure 8 and Figure 9, consisting of steady state pressures and temperatures and the ability to add high response unsteady pressure Kulite sensors.

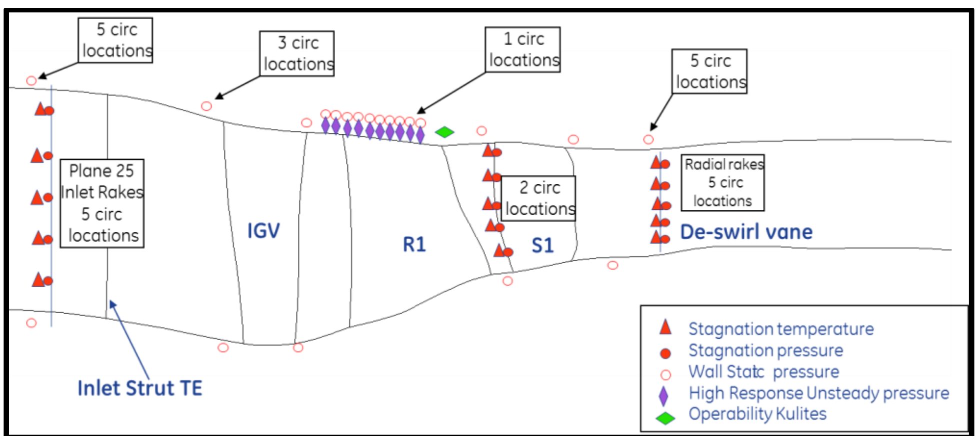

Figure 8 Inter-Stage Aero Instrumentation – 1-Stage Configuration

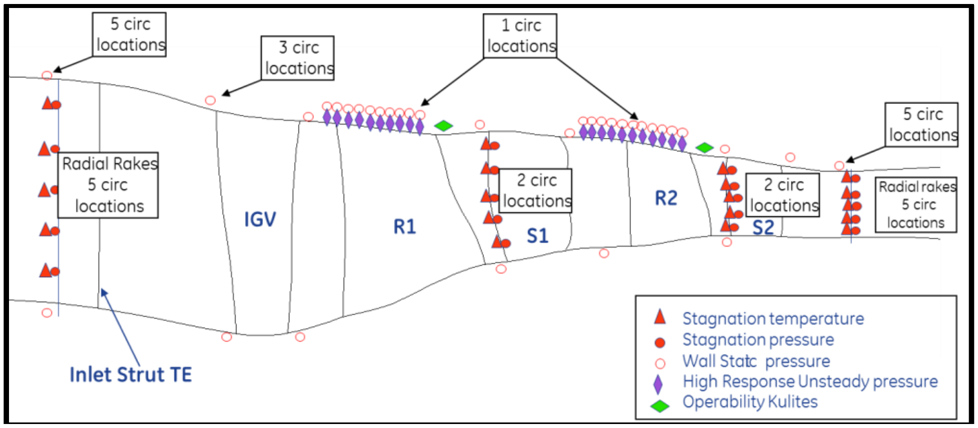

Figure 9 Inter-Stage Aero Instrumentation – 2-Stage Configuration

Table 2 Stator Leading Edge Instrumentation Immersion

	S1 LE	S2 LE
Immersion A	6.1%	9.4%
Immersion B	24.3%	28.2%
Immersion C	43.7%	47.5%
Immersion D	64.5%	67.4%
Immersion E	86.8%	88.1%

On the hub and casing for both configurations there are wall statics upstream and downstream of the IGV and each stator row. Also on the Stator LE, there are both stagnation pressure and stagnation temperature measurements at the immersions specified above in Table 2

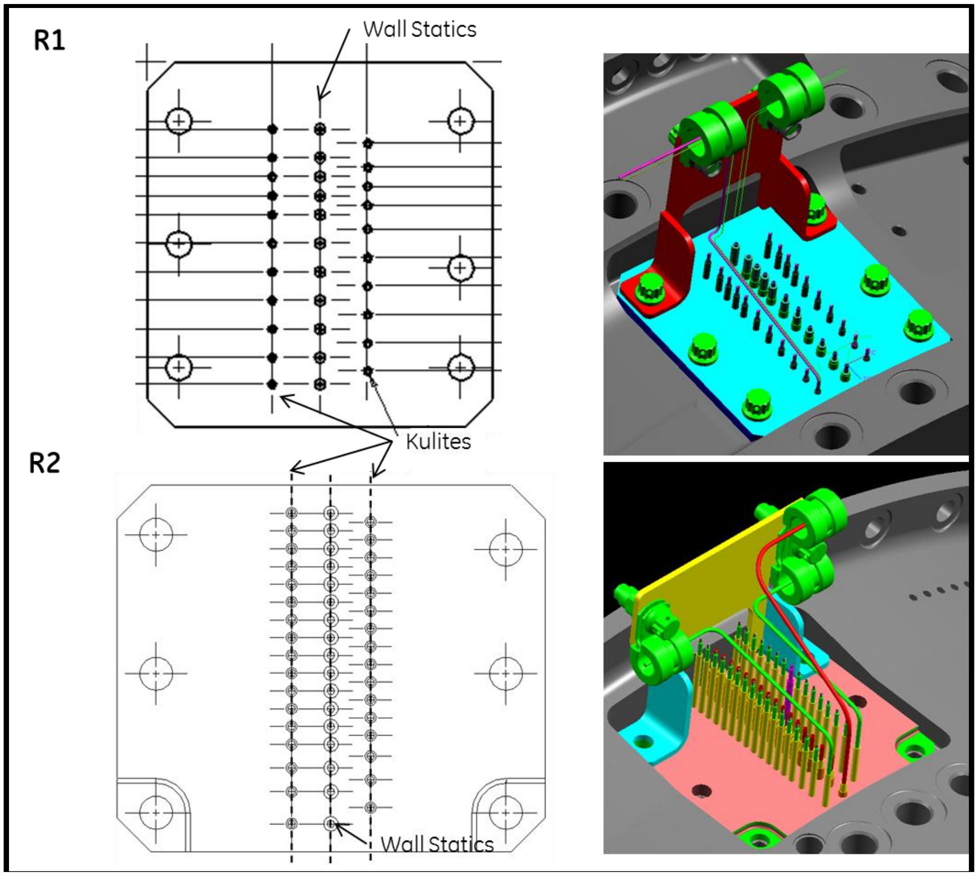

Figure 10 Over-the-Rotor Kulite Block

The test rig also has over the rotor (OTR) Kulite blocks, shown in Figure 10, that can be installed over both R1 and R2. These OTR blocks consist of an axial row of static pressure taps to measure the steady static pressure levels and 2 rows of high response Kulites that are capable of measuring the unsteady pressure over the rotor. Relating the signal with the rotor passing frequency provides a detailed view of the rotor static pressure field.

Test Plan

Both the 1-stg and 2-stg configuration consisted of three phases of testing: mechanical checkout, speedline mapping and traversing. Mechanical checkout consisted of determining that all the rig systems were working and clearing the rig of any dynamic risk in the intended operating range.

Speedline mapping was performed using 3 VSV settings at 2 speeds, 97% NC and 100% NC. The speedlines started below the opline and throttled up close to stall.

The 3 VSV settings were chosen to get loading derivatives on R1, S1, and R2 (on the 2-stg configuration). The VSV settings tested were the nominal VSV setting (designated condition N), IGV open 5 degrees (designated condition I) and IGV open 5 degrees with S1 closed 5 degrees (designated condition IS). The VSVs set to the "I" condition load up R1, while set to the "IS" condition, the VSVs load up R1 and unload S1 in both the 1-stg and 2-stg configuration as well as unload R2 in the 2-stg configuration.

Besides the standard pressure and temperature data collected with the fixed rakes, the stator LE instrumentation, and the wall taps, data was also acquired during the speedline mapping with the over the rotor (OTR) Kulite blocks on both the 1-stg and 2-stg configuration and with the exit wiper rake in the 2-stg configuration. The OTR Kulite blocks contained both static pressure taps and Kulites that give both the steady and unsteady static pressure across the entire rotor tip on both R1 and R2 (in 2-stg configuration).

The wiper rake contains 5 radial immersions and it was traversed circumferentially behind S2 acquiring PT and TT data across one S2 pitch.

Table 3 Traverse Conditions

Condition	% Corrected Speed	IGV	S1	Description
97N	97%	0	0	Nominal VSV schedule, intended opline pressure ratio
97I	97%	-5	0	IGV open 5 degrees, same opline as 97N
97IS	97%	-5	5	IGV open 5 degrees, S1 closed 5 degrees, same opline as 87N
97NL	97%	0	0 (-4*)	Nominal VSV schedule (* 2-stg had to open S1 4 degrees to get same opline), low opline R1 peake efficiency point
100N	100%	0	0	Nominal VSV shcedule, intended opline pressure ratio

The traverse phase of testing consisted of different traverses at 5 locations at 5 different conditions. The conditions chosen to traverse are shown above in Table 3 Traverse Conditions.

The traverses were conducted upstream of the strut, the IGV TE, the R1 TE, the S1 TE, and the R2 TE in the 2-stg configurations

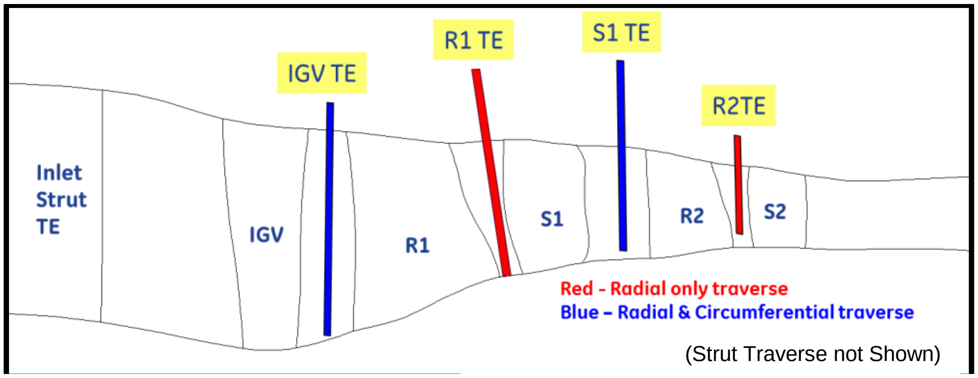

Figure 11 Approximate Traverse Locations

Table 4 Traverse Axial and Radial Locations

	Strut LE	IGV TE	R1 TE	S1 TE	R2 TE
Axial Location	0.88 chords upstream strut	0.35 chords downstream IGV	0.10 chords downstream R1	0.35 chords downstream S1	0.08 chords downstream R2
Immersions	2.5%	X	2.5%	X	2.5%
	3.7%	X	3.7%	X	3.7%
	5.0%	5.0%	5.0%	5.0%	5.0%
	7.5%	X	7.5%	X	7.5%
	10.5%	10.8%	10.5%	10.8%	10.5%
	20.0%	20.0%	20.0%	20.0%	20.0%
	31.7%	31.7%	31.7%	31.7%	31.7%
	40.0%	X	40.0%	X	40.0%
	51.9%	51.9%	51.9%	51.9%	51.9%
	60.0%	X	60.0%	X	60.0%
	71.6%	71.6%	71.6%	71.6%	71.6%
	80.0%	X	80.0%	X	80.0%
	90.5%	90.7%	90.5%	90.7%	90.5%
	92.5%	X	92.5%	X	92.5%
	95.0%	95.0%	95.0%	95.0%	95.0%
	96.2%	X	96.2%	X	96.2%

As Figure 11 shows, there were two types of traverses performed: radial only, as well as radial and circumferential. The radial only traverses consisted of 16 radial immersions, while the radial and circumferential traverses consisted of 28 to 30 circumferential locations at 8 radial immersions, shown above in Table 4.

There were four different traverse measurement types performed during the test. The X-wire probe was used upstream of the strut primarily to measure turbulence intensity and as much of the boundary layer as possible. Also a slant wire was traversed behind the S1 TE. By rotating the slant wire to 3 different angles, and ensemble averaging, the slant wire gives the 3-D flow field as a function of both time and space. The 5 hole probe gives the PT, TT, PS and 3 components of velocity, and the Kulite probe gives both steady state PT as well as the unsteady PT.

Table 5 Traverse Summary

			1 - Stg Configuration					2 - Stg Configuration				
Location	Measurement	Traverse Type	97N	97NL	97I	97IS	100N	97N	97NL	97I	97IS	100N
Strut	5 Hole	Radial Only	97N	X	X	X	100N	X	X	X	X	X
	X-Wire	Radial Only	97N	X	X	X	100N	X	X	X	X	X
IGV TE	5 Hole	Circumferential	97N	97NL	97I	X	100N	X	X	X	X	X
	Kulite	Circumferential	97N	97NL	X	X	X	X	X	X	X	X
R1 TE	5 Hole	Radial Only	97N	97NL	97I	97IS	100N	97N	97NL	97I	97IS	100N
	Kulite	Radial Only	97N	97NL	97I	97IS	100N	97N	97NL	97I	97IS	100N
S1 TE	5 Hole	Circumferential	97N	97NL	97I	97IS	100N	97N	97NL	97I	97IS	100N
	Kulite	Circumferential	97N	97NL	97I	97IS	100N	97N	97NL	97I	97IS	100N
	Slant-Wire	Circumferential	97N	97NL	97I	97IS	X	97N	97NL	97I	97IS	100N
R2 TE	5 Hole	Radial Only	N/A	N/A	N/A	N/A	N/A	97N	97NL	X	97IS	100N
	Kulite	Radial Only	N/A	N/A	N/A	N/A	N/A	97N	97NL	97I	97IS	100N

Table 5 above shows the summary of the traverses that were performed during the test. The strut and IGV traverses were performed on the 1-stg configuration only because their results are assumed to be independent of the addition of the 2nd stage to the test article. Likewise 97IS at the IGV TE was omitted since changing S1 angle in the 1-stg configuration had little to no effect on the flow through the compressor.

Results

Mechanical Checkout – Rotor Dynamics

The subject testing of this effort is a retest of the Tech56 HPC compressor front block, which had been successfully accomplished under a contract with the VAATE I Contract with AFRL (F33615-03-D-2352 Delivery Order 008) and reported under Final Report AFRL-PR-WP-TR-2009. The focus of mechanical checkout under this program activity was toward the rotor dynamics of the rig in the 1 and 2 stage configurations inclusive of hardware to interface with the NASA Glenn Research Center W7 test facility. Figure 12 shows the rig configuration and nomenclature in the NASA W7 test facility.

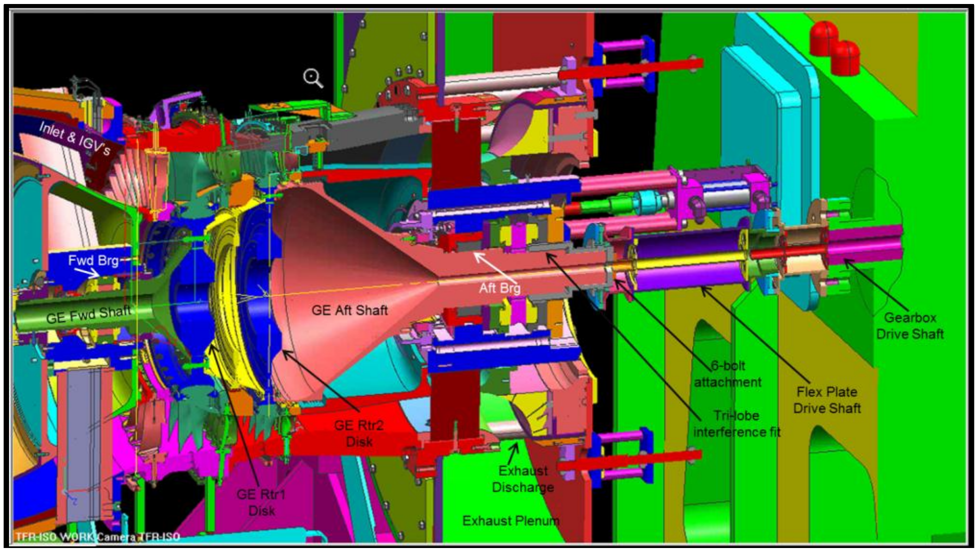

Figure 12 Tech56 Rig – Cutaway in NASA W7 Test Facility

During the assembly process, the rig rotor was balanced in both the 1-stg and 2-stg configurations. The 2-stg configuration was balanced with the resultant stg 2 blades and their locations marked for re-assembly. Following the 2-stg configuration balance, the 1-stg configuration was balanced with "dummy blades" in place of the 2 stg blades. The "dummy" blades were configured to replicate the flow-path in the absence of a 2nd stage of rotor airfoils. The "dummy" blades included features to allow the ability to be removed in such a way as to support re-assembly in-situ in the W7 facility. The rig was provided to NASA in the 1-stg w/ "dummy" blade configuration.

NASA provided instrumentation in the facility bearing hardware in response to GE rotor dynamics analyses.

System balance efforts during mechanical checkout supported the program objectives in clearing the rig for the subject aerodynamic testing in both the 1 stg and 2 stg rig configurations.

A brief post-test analysis of data taken during mechanical checkout efforts, produced a summary of conclusions and recommendations to support potential follow-on test programs in the W7 facility.

Results

1. Facility drive gearbox maximum response was ~0.3 ips-pk and had no critical peaking.
2. Trim balance at the forward plane (Stg1 blade base) reduced shaft motion at higher speeds to less than ½ mil-pk.
3. Test run on 6/22/13 had shifting (up to 2x) prox readings but steady vibes during trim runs.
4. The GE trims were done using multibal program with input from all four rig rotor proximity probes at 4 speeds.
5. Spectral analysis of the bearing prox probes shows the 1/rev content comprising ~99% of the amplitude signal with trace 2/rev and some spattering of higher power ½ per rev.

Conclusions and Recommendations:

1. Test results of rotor translation and pitch mode agree well with pre-test analysis
2. Facility gearbox response indicates low shaft unbalance with the confirmation that it's shaft modes were well above rig top speed.
3. Three or four trims (2 by NASA on aft plane and 3 by GE on forward plane) eliminated elevated rig rotor motion. Multibal should be used as the balance tool in future rig builds.
4. Multibal sensitivity, as expected, was maximum at the two speeds closest to the two rigid rotor modes.
5. Increasing bearing oil pressure improved stability, conclusion is higher pressure equals more efficient damping.
6. For the next phase buildup, install dynamics check points of the key rotor build steps.

Aerodynamics

1 Stg Rig Configuration - Mapping

Speed-line mapping was performed at 2 different speeds, 97% NC and 100% NC, and with 3 different VSV settings corresponding to the traverse conditions shown in **Error! Reference source not found.**. The names of the speedline correspond to he traverse point located on the speedline, for example, 97I contains the 97I traverse point and was performed with the VSV setting of IGV open 5 degrees. The 97NL point lies on the same speedline as the 97N point, but on a lower opline.

During the course of testing, conditions were set based on the pressure ratio across R1 using the S1 LE instrumentation. This method was chosen over using the exit rakes to set the condition for compatibility to previous and future testing, as well as to the 2-stg configuration, where there are no pressure and temperature instrumentation between the S1 TE and R2 LE.

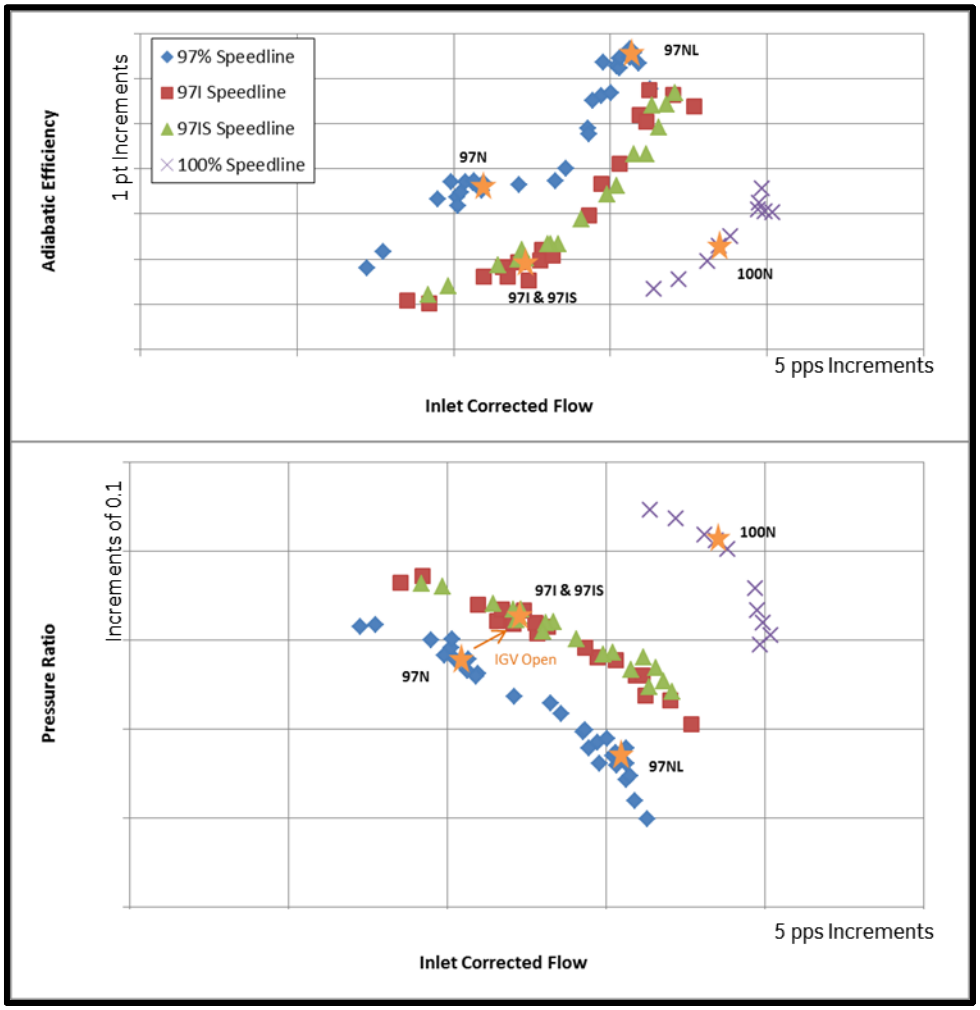

Figure 13 Compressor Map – 1-Stage Configuration, Plane 25 to S1 LE

The speedlines for the 1-stg configuration are shown in Figure 13. Loading up R1 by opening the IGV causes the rotor to move along its opline, and corresponds to a drop in efficiency of greater than 1.5 pts. The 97N and 100N points were based on the opline pressure ratio from the Tech 56 rig 3. However, the Tech 56 rig 3 had a different gooseneck/inlet duct that had much more loss than was bookkept into the target pressure ratio. This rig has little gooseneck/inlet duct loss, so when the Tech 56 rig 3 pressure ratios were targeted, the rig ran at a higher opline. The 97I and 97IS points resulted from the VSV changes from the 97N condition. The 97NL point is the peak efficiency point at 97% NC, and is at a point on an opline lower than the multi-stage machine can achieve with its current stage mapping.

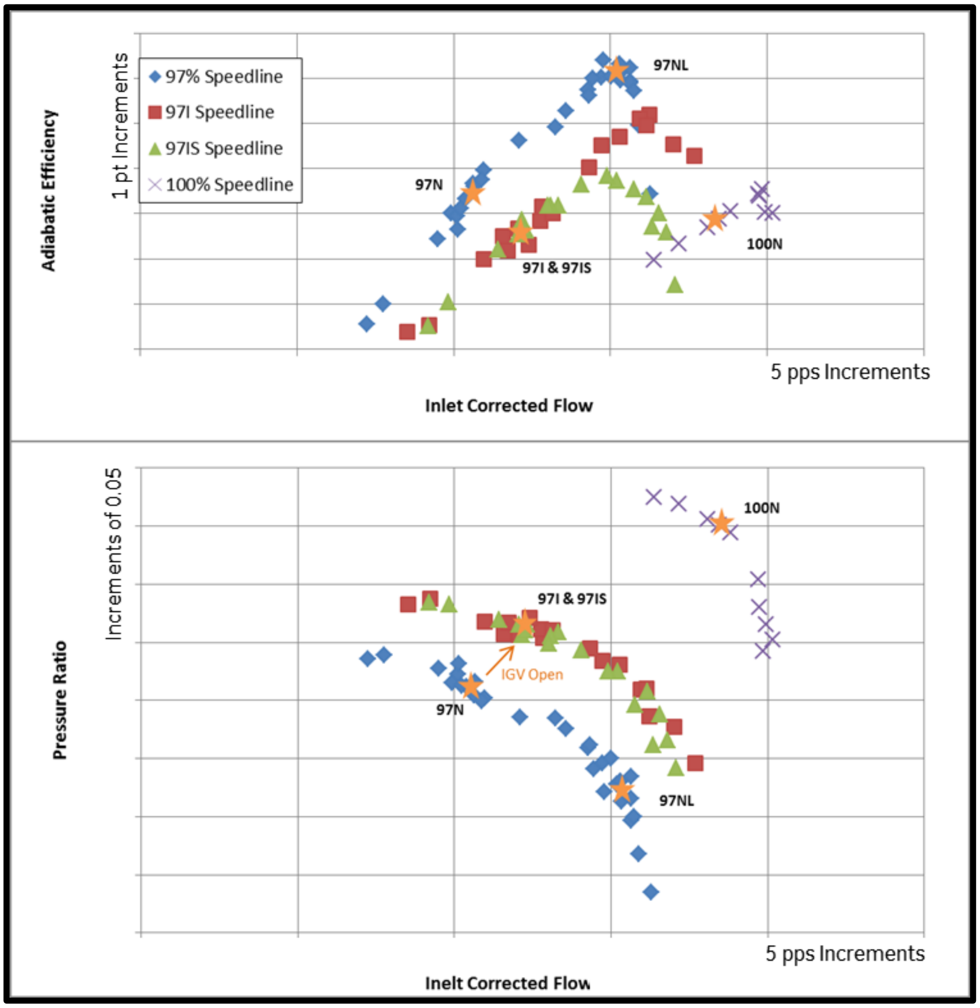

Figure 14 Compressor Map – 1-Stage Configuration, Plane 25 to Plane 30

The speedline map for the entire stage includes the additional losses due to the presence of S1 and is shown in Figure 14. Overall the stage map shows very similar trends to the R1 map. On the 97% speed line, the R1 map shows an inflection point that is not present in the stage map. This characteristic was repeatable on test, and maybe a result of instrumentation locally back pressuring the rotor.

1 Stg Rig Configuration - Traverse

Traverses were taken at 4 locations in the 1-stg configuration: ahead of the strut as shown in Figure 3 behind the IGV TE, behind the R1 TE, and behind the S1 TE as were shown in Figure 11.

The traverses behind the IGV measure the flow characteristics going into R1, and are important in breaking out the losses and understanding the R1 boundary conditions. Typical compressor instrumentation does not pick up the loss caused by the strut, gooseneck, and IGV up stream of the R1, instead this loss is usually assumed based off an analytical model, resulting in some uncertainty in rotor performance. With the goal of this test being the determination of where the loss occurs in these high stage loading machines and by what mechanism causes this loss, it is important to be able to break out the strut, gooseneck, and IGV loss from that of R1.

A 5-hole probe was traversed circumferentially at 8 radial locations, across 1.7 pitches of the IGV containing 2 IGV wakes, with one of the IGV wakes also containing the strut wake. From these 2 wakes, the loss due to the strut and the IGV were determined and then used to guide the loss input into our 2-D throughflow model, CAFMIX.

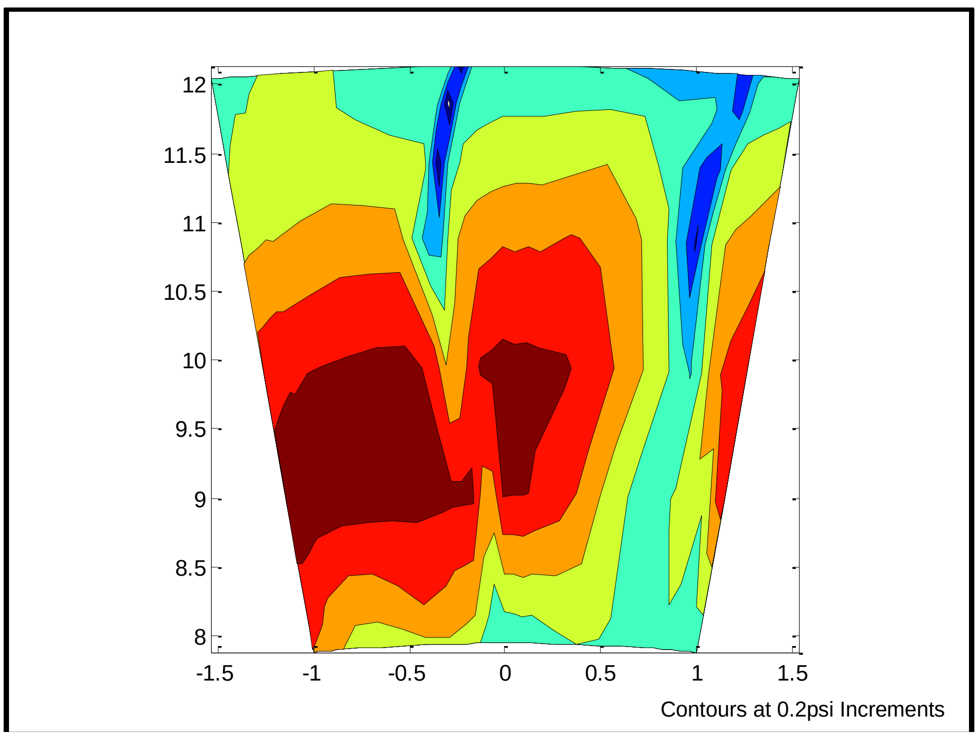

Figure 15 Total Pressure Contour Behind IGV @ 97NL

The total pressure contours from the 5-hole probe in Figure 15 contain 2 IGV wakes with the wake on the right containing the wake from the upstream strut as well. By area averaging across the left wake, the pressure loss of the IGV can be determined, and by area averaging across the right wake, the loss of the combination of the IGV and strut is determined.

Figure 16 shows the area average of the IGV only wake, the IGV and strut wake, and a compilation of the two to give an average inlet into R1. The IGV only area average is represented by the red line which has the highest total pressure. The addition of the strut wake with the IGV yields the lowest average total pressure and is shown in blue. An average inlet was computed by taking the weighted average of 5 IGV with strut wake and 37 IGV only wakes.

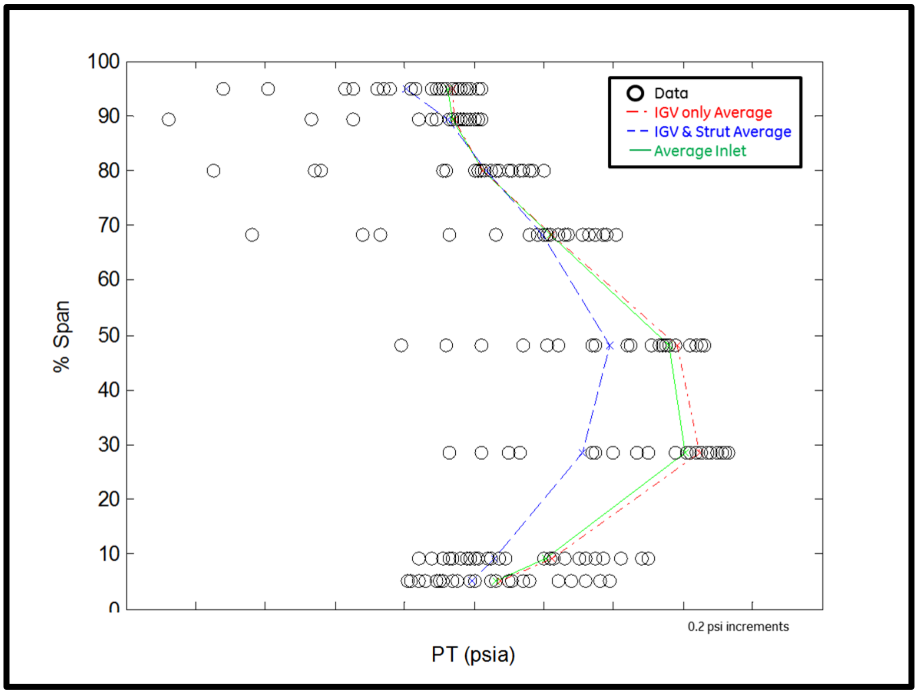

Measurements scaled to same inlet conditions

Figure 16 Area Avg Total Pressure – IGV, IGV& Strut, Compiled Average Inlet @ 97NL

Using the same approach as the total pressure, the average meridional swirl angle can be computed by averaging the 3 components of velocities acquired by the 5-hole traverse, and is shown in Figure 17.

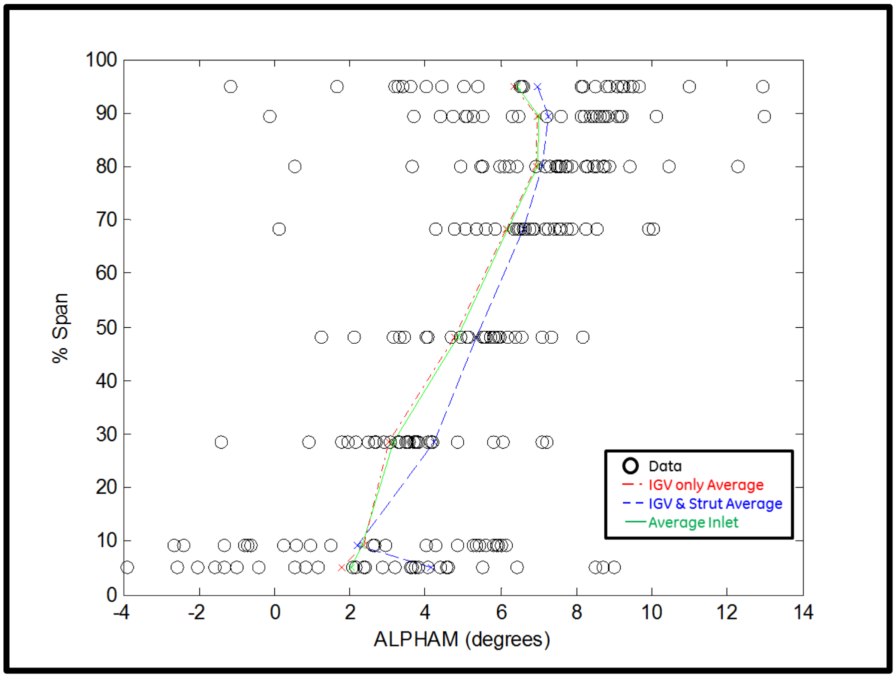

Figure 17 Area Avg Meridional Swirl – IGV, IGV & Strut, Compiled Average Inlet @ 97NL

The traverse behind the R1 TE was used as an independent measurement from the S1 LE instrumentation. Both 5-Hole and Kulite probes were traversed radially behind R1 at 16 different immersions, with the 5-hole probes giving average PT, PS, TT, and 3 components of velocity and the Kulite probes giving both time average and unsteady PT.

Figure 18presents the Total and Static Pressure behind R1 TE from S1 LE instrumentation, 5-hole & Kulite traverses and CAFMIX flow model at 97NL. Also included is an estimate of total pressure from mid passage values at S1 TE from 5 hole & Kulite traverses and exit rakes.

The 5 hole traverse and the Kulite traverse agree well with each other for the time averaged total pressures when scaled to the same inlet conditions.

This good agreement is seen in Figure 18, where at each immersion, there are 2 red symbols, with one of them being the 5-Hole traverse and the other being the Kulite traverse. Throughout most of the span they line up almost on top of each other. Overall both the 5 hole and Kulite traverses read higher pressures than the S1 LE instrumentation, especially in the hub.

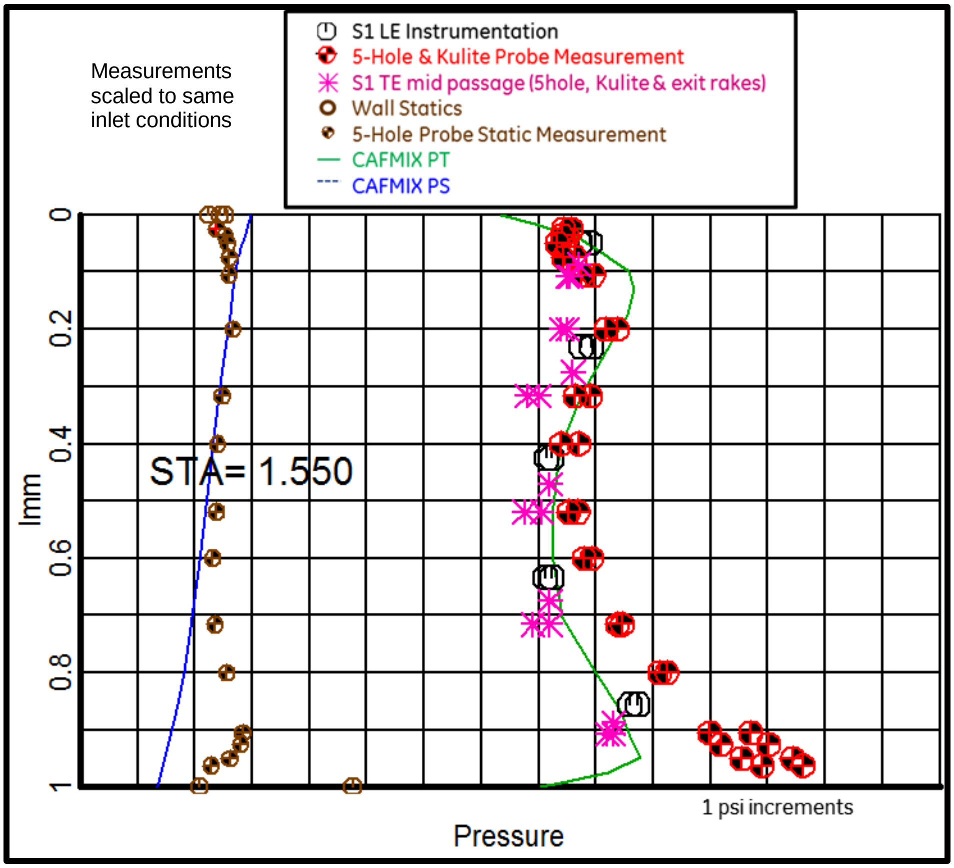

Figure 18 R1 TE Total and Static Pressure Behind R1 TE @ 97NL

Figure 19 presents the total temperature behind R1 TE from S1 LE instrumentation, 5-hole traverse and CAFMIX flow model at 97NL. Also included is an area average of S1 TE total temperature from 5 hole traverse and exit rakes.

The 5hole traverse total temperature data shown in Figure 19, has a similar shape as the S1 LE instrumentation, but reads higher in the tip region. However, both the 5-hole traverse and the S1 LE instrumentation read a higher temperature than measured downstream of the S1 TE by a 5 hole traverse and the exit rakes. The resulting average temperature is significantly higher than the temperature measured at the S1 TE. Since the flow is going through a stator, there should be no appreciable change in temperature.

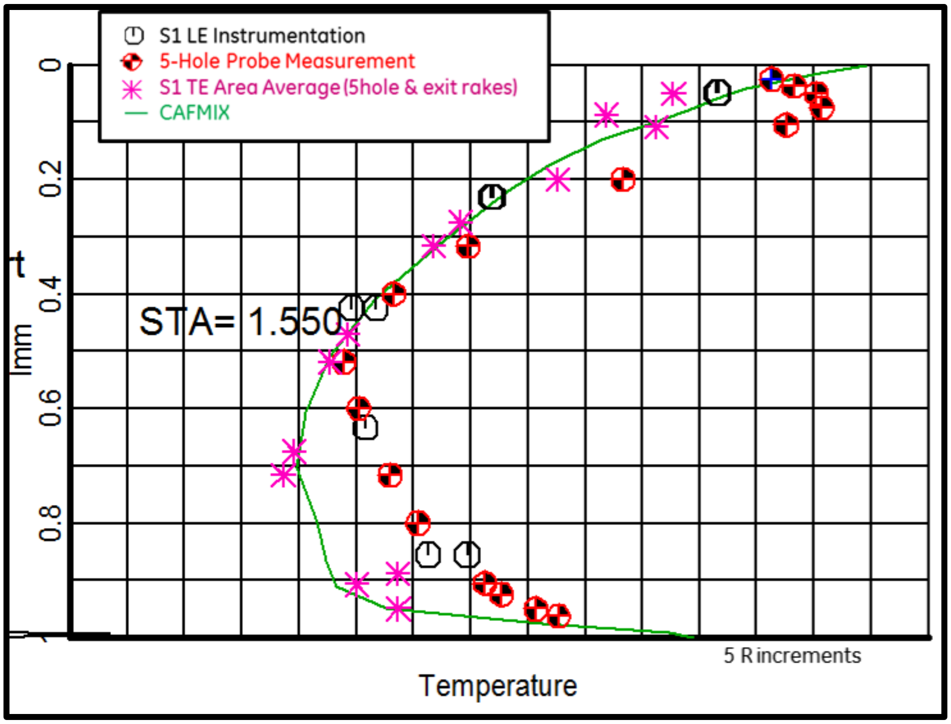

Measurements scaled to same inlet conditions

Figure 19 Total Temperature Behind R1 TE from S1 @ 97NL

The traverse data appears to be reading high in both total pressure and temperature, with the hub reading higher than the casing. One possible explanation is that the traverse itself creates blockage that locally back pressures the rotor. This causes the rotor to throttle up, resulting in a higher reading in pressure and temperature. As the traverse extends further into the passage, it creates more blockage, affecting the traverse measurement at the hub more than the case. When the mid passage pressures from the 5-hole, Kulite, and exit rakes are plotted in the magenta color in Figure 18, they show a lower pressure than the S1 LE instrumentation, implying that the S1 LE instrumentation is causing local back pressuring of the rotor.

5-hole and Kulite probes were traversed across approximately a stator pitch at 8 immersions resulting in a measurement of PT, PS, TT and 3 components of velocity from the 5-hole probe and both time average and unsteady PT from the Kulite probe.

A total pressure trace from the 5-Hole and Kulite traverses at 68.3% span at 97NL from S1TE 5-Hole and Kulite traverses is shown in Figure 20. Shown for comparison are the upstream R1TE measured values, and estimated mid-passage average values. As shown, the total pressure measured upstream of the stator does not agree with the total pressure measured downstream of the stator.

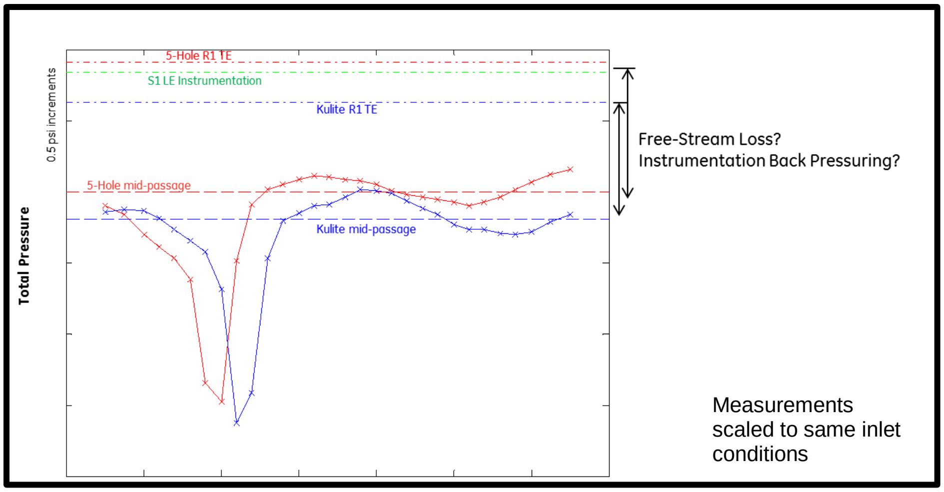

Figure 20 Total Pressure at 68.3% Span @ 97NL

The 5-hole and Kulite traverses taken at the S1 TE agree with each other in level and overall shape, but are at a significantly lower pressure than the time average measurements taken upstream of the S1 LE. When comparing to the upstream pressure to a mid-passage average downstream pressure, there is a significant amount of implied free-stream loss. This loss would influence all of the flow coming into the stator, not just in the stator boundary layer, wake, and secondary flow regions.

If the measurements upstream of the S1 LE are reading artificially high, due to local back-pressuring of the rotor, then the rotor pressure ratio would be lower indicating that the loss is really in the rotor, and not in the free stream of the stator. The discrepancy in the pressure measurements would then be explained by this local back pressuring.

The CAFMIX datamatch had difficulty matching the R1 TE temperatures and required large amount of empiricism to adjust CAFMIX's physics model, and if R1 TE temperatures were matched, the model could not also match the S1 TE temperatures. However, when the CAFMIX was matched to the S1 TE temperatures the required empiricism was much more reasonable. Also, when running a very initial R1 CFD calculation, the CFD temperature results compared much better to the S1 TE match than the R1 TE match temperatures.

The 5-hole and Kulite probe traverse both show similar results in pressure trace in Figure 20 and the total pressure contours shown in Figure 21. The contour plots both show the S1 wake and in the bottom right, they also show the S1 endwall clearance vortex.

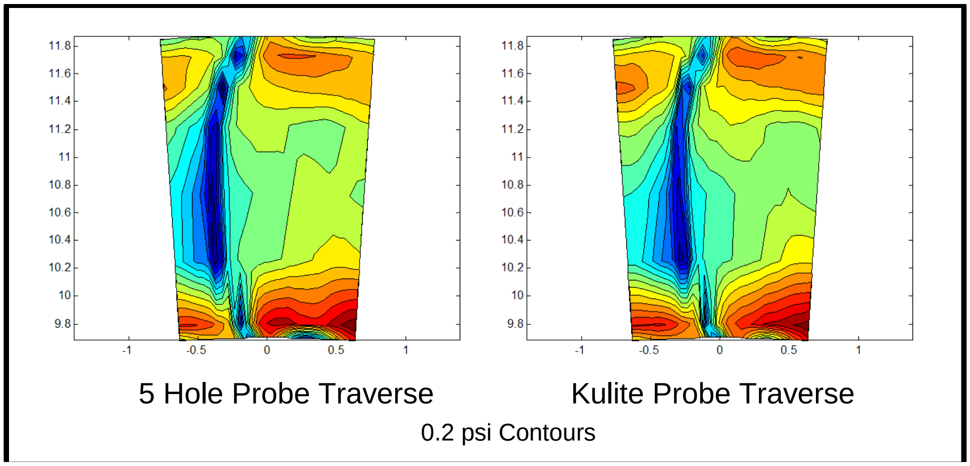

Figure 21 S1 TE Total Pressure Contours @ 97NL

Figure 22 and Figure 23 show the circumferential total pressure from the 5-hole traverse behind the S1 TE at 48.1% and 68.3% span during the 97NL condition. The total pressure plot shows the S1 wake, and lower pressure along the pressure side of the airfoil outside of the wake (left of the wake on the plot).

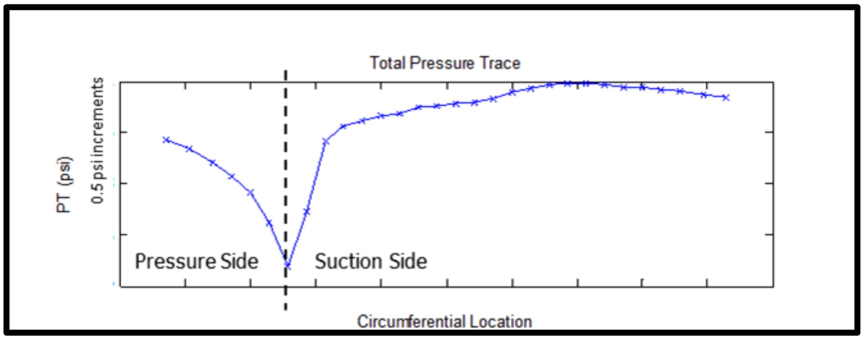

Figure 22 S1 TE Total Pressure at 48.1% Span @ 97NL

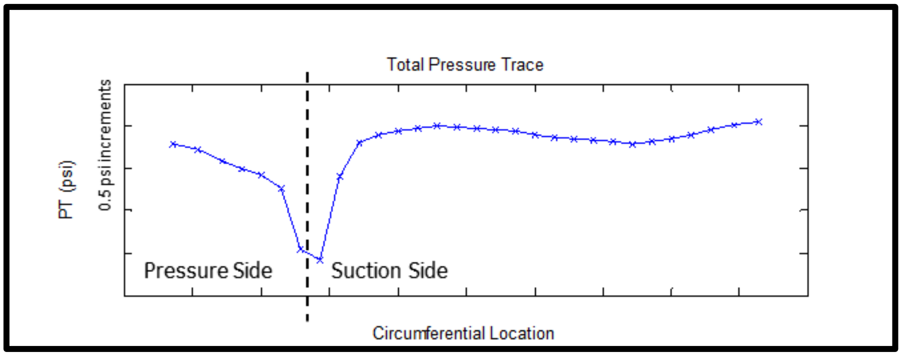

Figure 23 S1 TE Total Pressure at 68.3% Span @ 97NL

Figure 24 and Figure 25 show the circumferential total pressure traces from the 5-hole traverse behind the S1 TE at 48.1% and 68.3% span during the 97N condition. The total pressure trace shows the S1 wake.

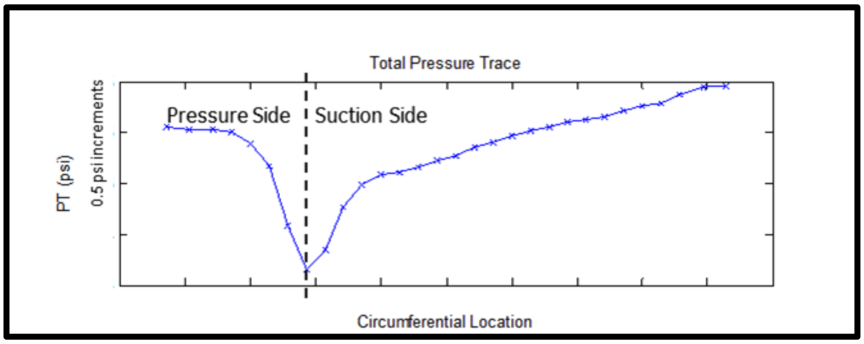

Figure 24 S1 TE Total Pressure at 48.1% Span @ 97N

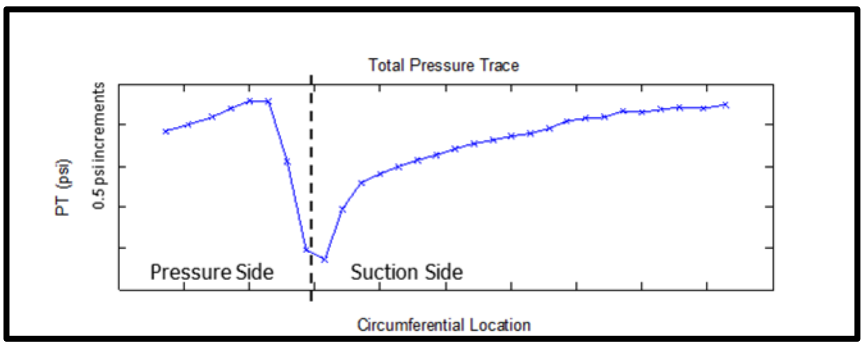

Figure 25 S1 TE Total Pressure at 68.3% Span @ 97N

The unsteady pressure from the Kulite trace shows the rotor wake passing through the stator.

The time space plots in Figure 26 and Figure 27 show the stator wake as a region of low pressure, highlighted by the dashed line. The stator wake shows some wobbling but is mainly pretty constant in space as would be expected. At a given circumferential location, the rotor wake passes through at the R1 blade passing frequency.

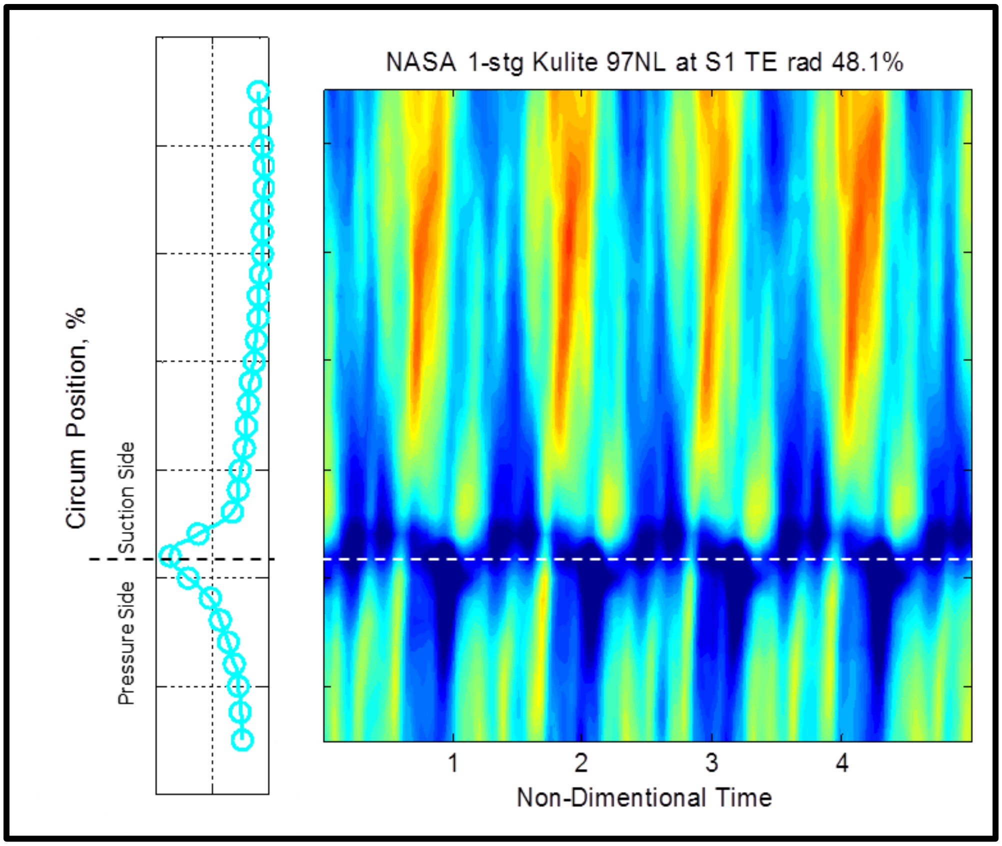

Figure 26 Time-Space Plots of Total Pressure at 48.1% Span @ 97NL

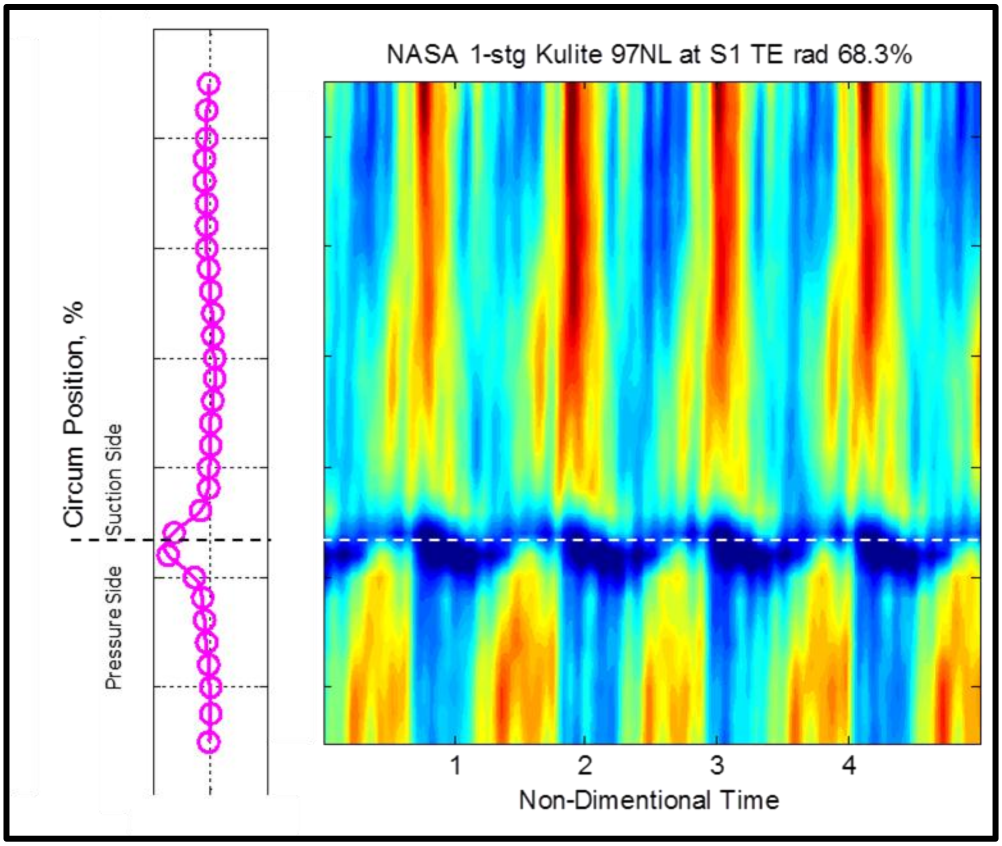

Figure 27 Time-Space Plots of Total Pressure at 68.3% Span @ 97NL

2 Stg Rig Configuration - Mapping

Speedline mapping was performed at the same conditions as the 1-stg configuration, at 2 different speeds, 97% NC and 100% NC, and with 3 different VSV settings at 97% Speed and 100% speed, consisting of nominal (condition N), IGV open 5 degrees (condition I), and IGV open 5 degrees with S1 closed 5 degrees (condition IS).

During the course of testing, conditions were set based off of the pressure ratio across R1 using the S1 LE instrumentation to match the conditions set in the 1-stg testing. There are no rakes at the S1 TE in the 2-stg configuration

The speedlines for the 2-stg configuration is shown in Figure 28, shows that the peak efficiency point is between the 97N and 97NL point. In order for the 2-stg compressor to reach the 97NL point, S1 had to be opened 4 degrees, loading up R2, otherwise the compressor could not pass enough flow. Loading up R1 by moving the IGV causes the rotor to move along its opline, and results in an overall no change in efficiency since R2 is improving as R1 declines. Closing S1 5 degrees with the IGV opened 5 degrees, drops the pressure ratio but increases the efficiency almost 2 pts.

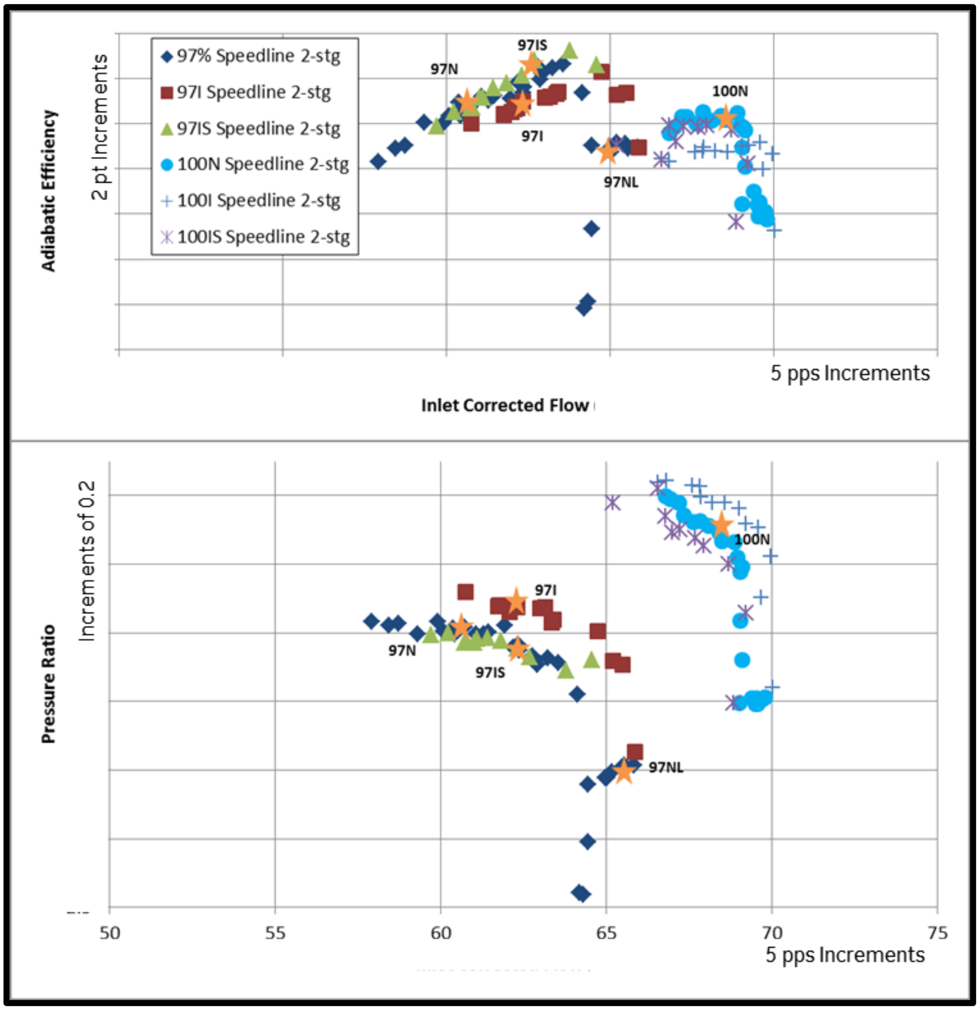

Figure 28 Compressor Map – 2-Stage Configuration, Plane 25 to Plane 30

Comparing the 2-stg R1 map to the 1-stg test, as shown in Figure 29, shows that for the 97N, 97I, and 100N speed lines, there is no change in R1 performance. The 2-stg speedlines are directly on top of the 1-stg speedlines. Closing S1 5 degrees for the 97IS speedline, generally shifts the speedline along the 97I as R1 is throttled by the reduced pumping in R2. This combination shows higher efficiency; however, more investigation is needed to determine if the change in stator angle causes the LE instrumentation to backpressure the rotor differently resulting in a different measurement.

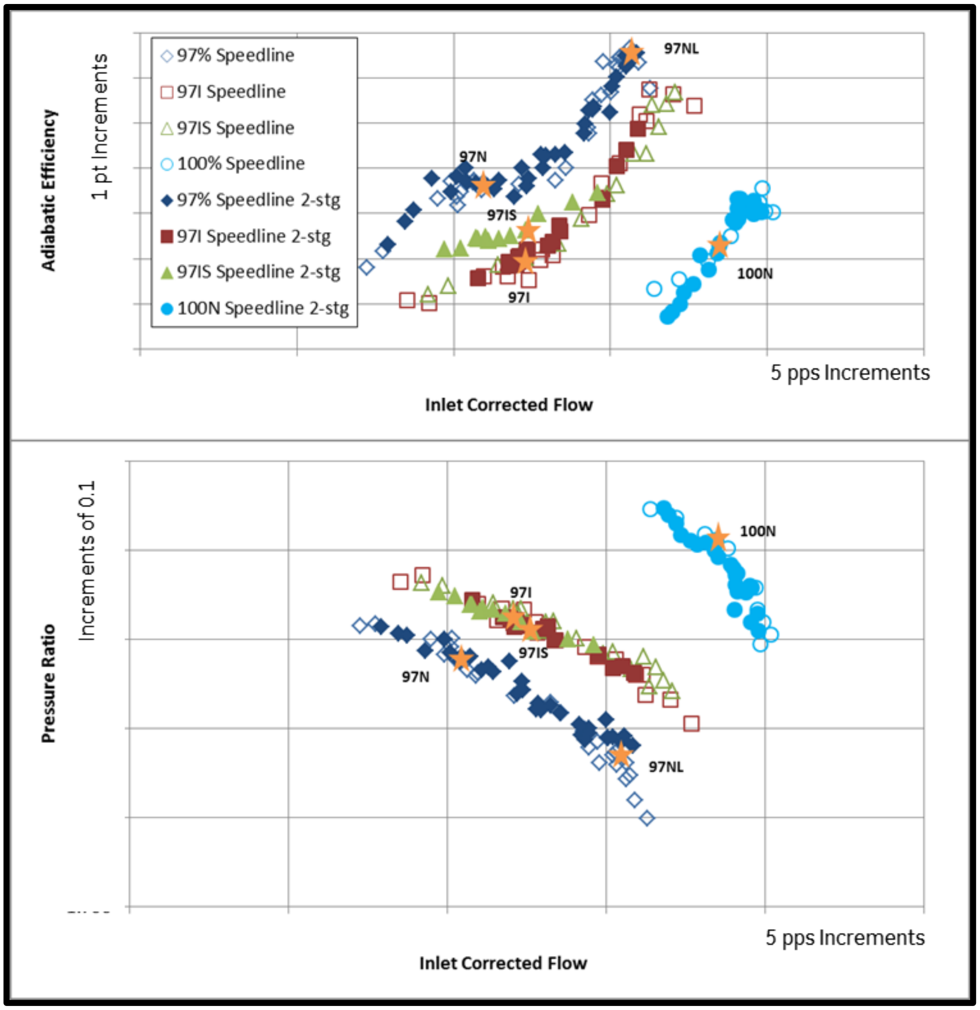

Figure 29 Compressor Map – 2-Stage Configuration, Plane 25 to S1 LE

The mapping shows that the 1-stg and 2-stg configurations have no effect on the first stage performance.

Traverses were also performed in the 2-stg configuration behind both rotors and behind S1. There were also wiper rake measurements taken behind S2 during the mapping phase of testing. The initial datamatch of the 97N point in the 2-stg configuration uses the same empiricism as the 1-stg configuration, meaning that the first stage in the 2-stg configuration behaves similarly to the first stage in the 1-stg configuration.

Since the loss is in both configurations, most of the investigation to date has focused on the 1-stg rig results.

Conclusions

The testing consisted of 2 configurations, a 1 stage configuration, and a 2 stage configuration, in order to separate out the source of high losses. For both configurations, detailed speedline mapping was performed at 97% and 100% speed, acquiring pressure and temperature data from LE instrumentation, wall statics, over the rotor Kulites, and in the 2-stg configuration, a wiper rake behind S2 TE. In addition to the mapping points, detailed traverses obtaining both time average and unsteady measurements were completed in 5 positions in the rig, obtaining a new reference set of data.

The 1-stg configuration showed that the loss is in the first stage of the compressor . Also seen during testing is that the traverses and possibly even the stator LE instrumentation can cause local back pressuring, which locally throttles the high stage loading rotor. Wall static pressure taps become instrumental in setting up the datamatch.

The 2-stg configuration testing shows that the loss is still present in this configuration, and no significant additional source of loss is observed as it behaves similarly to the 1-stg configuration.

Continuing Work

With the vast amount of high quality data that was taken during this test campaign, there is a large amount of continuing work to be completed beyond what was shown in this report to investigate the detailed loss sources and ultimately compare them to CFD modeling results. Some of the most immediate work that will be conducted involved looking in more detail to the unsteady Kulite data, and the steady and unsteady hotwire data, as well as the over the rotor Kulite blocks and further examination of the different loading effects due to VSV angles and a deeper look into the 2nd stage performance on the 2-stg configuration. The data set acquired from this test will also be used to validate CFD and help determine how to design for these loss mechanisms.

REPORT DOCUMENTATION PAGE

Form Approved
OMB No. 0704-0188

1. REPORT DATE *(DD-MM-YYYY)*	2. REPORT TYPE	3. DATES COVERED *(From - To)*
30 – 04 – 2014	Final	29 Sep 2010 - 30 April 2014

4. TITLE AND SUBTITLE

ERA Advanced Core Compressor Technology

5a. CONTRACT NUMBER
NNC10BA06B/NNC10TA64T

5b. GRANT NUMBER

5c. PROGRAM ELEMENT NUMBER

6. AUTHOR(S)

David Lurie, Andy Breeze-Stringfellow, Stuart Wilson, Richard Obear, Ki Sohn, Hyoun-Woo Shin

5d. PROJECT NUMBER

5e. TASK NUMBER

5f. WORK UNIT NUMBER

7. PERFORMING ORGANIZATION NAME(S) AND ADDRESS(ES)
GE Aviation
1000 Western Ave
Lynn, MA 01910

8. PERFORMING ORGANIZATION REPORT NUMBER
R2014AE332

9. SPONSORING/MONITORING AGENCY NAME(S) AND ADDRESS(ES)
NASA
Glenn Research Center
21000 Brookpark Road
Cleveland, OH 44135

10. SPONSOR/MONITOR'S ACRONYM(S)

11. SPONSORING/MONITORING AGENCY REPORT NUMBER

12. DISTRIBUTION AVAILABILITY STATEMENT
Unlimited

13. SUPPLEMENTARY NOTES
None

14. ABSTRACT

As part of the NASA Integrated Systems Research Program, Environmentally Responsible Aviation Project, NASA GRC and GE Aviation have partnered to investigate the technology barriers associated with improved fuel economy of large gas turbine engines. Crucial to improving fuel economy is the increase in Pressure Ratio (PR) of the core compressor.

This goal of this work is to provide a dedicated component test vehicle to study the very challenging compressor front stage performance and operability issues that arise in these aggressive machines. With a view to providing highly detailed aerodynamic data that provides an industry standard data set for CFD validation.

15. SUBJECT TERMS
High Pressure Ratio Compressor, Front Block, Aerodynamic Performance, ERA, NASA GRC, GE Aviation

16. SECURITY CLASSIFICATION OF: a. REPORT	b. ABSTRACT	c. THIS PAGE	17. LIMITATION OF ABSTRACT	18. NUMBER OF PAGES	19a. NAME OF RESPONSIBLE PERSON / 19b. TELEPONE NUMBER (*Include area code*)
Unclassified	Unclassified	Unclassified	Unlimited	33	**M. Celestina** / (216) 433-5938

INSTRUCTIONS FOR COMPLETING SF 298

1. REPORT DATE. Full publication date, including day, month, if available. Must cite at lest the year and be Year 2000 compliant, e.g., 30-06-1998; xx-08-1998; xx-xx-1998.

2. REPORT TYPE. State the type of report, such as final, technical, interim, memorandum, master's thesis, progress, quarterly, research, special, group study, etc.

3. DATES COVERED. Indicate the time during which the work was performed and the report was written, e.g., Jun 1997 - Jun 1998; 1-10 Jun 1996; May - Nov 1998; Nov 1998.

4. TITLE. Enter title and subtitle with volume number and part number, if applicable. On classified documents, enter the title classification in parentheses.

5a. CONTRACT NUMBER. Enter all contract numbers as they appear in the report, e.g. F33615-86-C-5169.

5b. GRANT NUMBER. Enter all grant numbers as they appear in the report, e.g. 1F665702D1257.

5c. PROGRAM ELEMENT NUMBER. Enter all program element numbers as they appear in the report, e.g. AFOSR-82-1234.

5d. PROJECT NUMBER. Enter al project numbers as they appear in the report, e.g. 1F665702D1257; ILIR.

5e. TASK NUMBER. Enter all task numbers as they appear in the report, e.g. 05; RF0330201; T4112.

5f. WORK UNIT NUMBER. Enter all work unit numbers as they appear in the report, e.g. 001; AFAPL30480105.

6. AUTHOR(S). Enter name(s) of person(s) responsible for writing the report, performing the research, or credited with the content of the report. The form of entry is the last name, first name, middle initial, and additional qualifiers separated by commas, e.g. Smith, Richard, Jr.

7. PERFORMING ORGANIZATION NAME(S) AND ADDRESS(ES). Self-explanatory.

8. PERFORMING ORGANIZATION REPORT NUMBER. Enter all unique alphanumeric report numbers assigned by the performing organization, e.g. BRL-1234; AFWL-TR-85-4017-Vol-21-PT-2.

9. SPONSORING/MONITORS AGENCY NAME(S) AND ADDRESS(ES). Enter the name and address of the organization(s) financially responsible for and monitoring the work.

10. SPONSOR/MONITOR'S ACRONYM(S). Enter, if available, e.g. BRL, ARDEC, NADC.

11. SPONSOR/MONITOR'S REPORT NUMBER(S). Enter report number as assigned by the sponsoring/ monitoring agency, if available, e.g. BRL-TR-829; -215.

12. DISTRIBUTION/AVAILABILITY STATEMENT. Use agency-mandated availability statements to indicate the public availability or distribution limitations of the report. If additional limitations/restrictions or special markings are indicated, follow agency authorization procedures, e.g. RD/FRD, PROPIN, ITAR, etc. Include copyright information.

13. SUPPLEMENTARY NOTES. Enter information not included elsewhere such as: prepared in cooperation with; translation of; report supersedes; old edition number, etc.

14. ABSTRACT. A brief (approximately 200 words) factual summary of the most significant information.

15. SUBJECT TERMS. Key words or phrases identifying major concepts in the report.

16. SECURITY CLASSIFICATION. Enter security classification in accordance with security classification regulations, e.g. U, C, S, etc. If this form contains classified information, stamp classification level on the top and bottom of this page.

17. LIMITATION OF ABSTRACT. This block must be completed to assign a distribution limitation to the abstract. Enter UU (Unclassified Unlimited) or SAR (Same as Report). An entry in this block is necessary if the abstract is to be limited.